International Journal of Informatics and Communication Technology (IJ-ICT)
Vol. 13, No. 2, August 2024, pp. 248~256
ISSN: 2252-8776, DOI: 10.11591/ijict.v13i2.pp248-256

A comprehensive analysis of dynamic PAPR reduction schemes in MIMO-OFDM systems

Ramadevi Dubala, P. Trinatha Rao
Department of Electronics Communication Engineering, GITAM University, Hyderabad, Telangana, India

Article Info

Article history:

Received Mar 1, 2024
Revised Apr 25, 2024
Accepted May 12, 2024

Keywords:

Decomposed Selective Mapping
Dynamic threshold-based logarithmic companding
MIMO OFDM
Modified enhancement asymmetric arithmetic coding
UFMC

ABSTRACT

In this paper, an attempt develops three different methods, namely, Hybrid Maximal-Minimum (Max-Min) model with Decomposed Selective Mapping (D-SLM) in a UFMC, Modified Enhancement Asymmetric Arithmetic Coding Scheme (M-EAAC) and Dynamic Threshold-based Logarithmic Companding (DTLC) is carried out in Multiple-Input, Multiple-Output Orthogonal Frequency-Division Multiplexing (MIMO-OFDM) technology to enhance the PAPR reduction. These methods allow increased data rate request through threshold limit adjustment in a desired out-of-band (OOB) range, allows data transmission for the selected for the candidate sequences for maximizing the channel utility, data capacity and computational demands and varying threshold limit to analyse the nonlinear companding effect, respectively on D-UFMC-SLM, M-EAAC SCS-TI and DTLC. The extensive analysis shows that the proposed M-EAAC SCS-TI achieves a reduced CCDF PAPR, increased average spectral efficiency and redued Bit Error Rate (BER) than the other proposed DTLC and D-UFMC-SLM methods.

Corresponding Author:

Ramadevi Dubala
Department of Electronics Communication Engineering, GITAM University
Hyderabad, Telangana, India
Email: dubalarama@gmail.com

1. INTRODUCTION

Scalable modulation and Multiple access with modifications in the network layer enable 5G networks to deliver max data rate (>30 Gb/s) [1], reduced energy limitations [2], enhanced service and ultra-reliable low latency [3] for industrial applications. Many sectors are slowly introducing 5G services to fulfill user needs [4]. Orthogonal frequency division multiplexing (OFDM) [5] with a cyclic prefix enhances inter-symbol interference (ISI) tolerance, which is the standard for future 5G networks [6]. This eliminates multi-path fading and maintained the intra-channel interference (ICI) tradeoff [7]. Its wide bands, inaccuracy in data synchronization, and high peak-to-average power ratio (PAPR) due to guard bands further reduce spectral efficiency [7]. Further, PAPR reduced offers a performance trade-off between the complexity and latency [8]. The near optimal performance makes the complexity to be similar with FFT estimations [9], where both Universal Filtered Multicarrier (UFMC) [10] and Multiple-Input, Multiple-Output OFDM (MIMO-OFDM) [11], a practically infeasible one.

To mitigate, such limitations, the objective of the proposed method is given: (i) To optimize desired out-of-band (OOB) range [12] using a weighting factor on PAPR reduction; (ii) To use appropriate PAPR minimization for maximizing the channel utility, data capacity and computational demands in MIMO-OFDM transmission; and, (iii) To analyse the effect of nonlinear companding [13]-[18] on PAPR reduction in MIMO-OFDM systems.

With these objectives, the following are the contributions of the research: (i) Depending on the first objective, the research developed a Hybrid Maximal-Minimum (Max-Min) model with Decomposed Selective Mapping (D-SLM) in a 5G UFMC (D-UFMC-SLM) for PAPR reduction. D-SLM sub-blocking accommodates the new data rate request by adjusting the tolerable limit of dynamic PAPR. (ii) Based on the second objective, a Modified Enhancement Asymmetric Arithmetic Coding Scheme (M-EAAC) is developed that reduces the high PAPR in sub-block OFDM candidate sequences [19]-[22]. It uses spatial circular shifting in temporal interleaving (SCS-TI) for diverse set generation of conjugated phases, which allows for the candidate sequence selection with the lowest PAPR for data transmission on MIMO-OFDM. (iii) Based on the third objective, a Dynamic Threshold-based Logarithmic Companding (DTLC) is developed for PAPR reduction in MIMO-OFDM [23]-[26]. The threshold limit is varied w.r.t the companding level under various companding level, which enhances the PAPR reduction.

The outline of the paper is given below: section 2 discusses the system model. Section 3 discusses the proposed methods including: (i) D-UFMC-SLM, (ii) M-EAAC SCS-TI, and (iii) DTLC. Section 4 provides comparative assessment of all the proposed methods over BER, PAPR reduction and average spectral efficiency (ASE), under various conditions. Section 5 concludes the work with possible directions for future scope.

2. SYSTEM MODEL FOR UFMC AND OFDM

2.1. UFMC Model

UFMC is a multi-carrier modulation to parallelly distribute higher data stream with slow data rate across the entire sub-bands of B band with sub-carriers Nb and available sub-carriers Nsc. N-point IFFT handles sub-band data, and filters have finite impulse response, and it converts sub-band data to UFMC prior wireless transmission based on the 5G UFMC architecture in Figure 1.

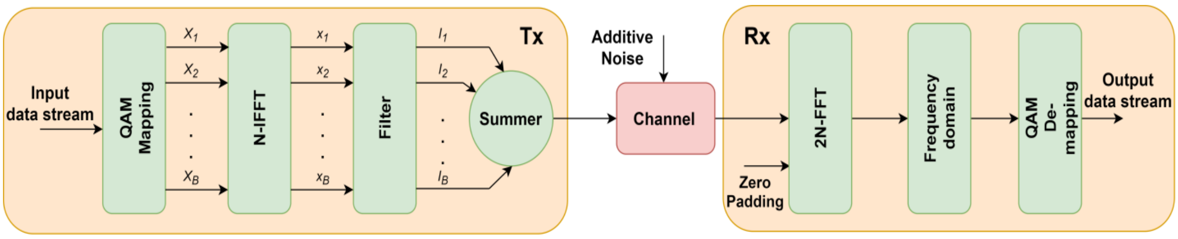

Figure 1. 5G-UFMC architecture

The transmitted signal $x = \sum_{b=1}^{B} F_b \bar{D} S_b$contains Toeplitz matrix Fb with FIR response, matrix elements $\bar{D} = \left[D_{cp} : D\right]^H$ and a singular vector quantity Sb of the transmitted signal at sub-band b. The received signal $y = \Re^{(N+L_f-1)\times 1}$is matched with transmitted signal.

2.2. MIMO Model

The MIMO-OFDM in Figure 2 contains an input stream (i.e., $Sinput = (S1, S2, \ldots, SN)$) with 'N' symbols, distributed independently and uniformly. Quadrature Amplitude Modulation (QAM) is utilized as the modulation scheme with N-carrier discrete-time OFDM signal.

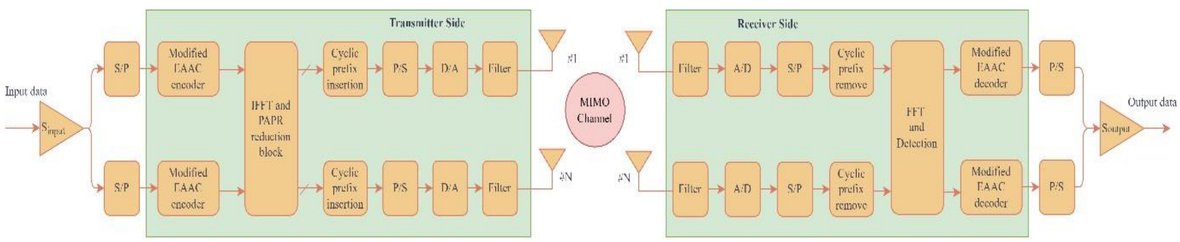

Figure 2. MIMO-OFDM block diagram

Same phase factors for large symbols in OFDM result in strong PAPR. Thus, the PAPR trade off analysis using central limit theorem needs a Gaussian distribution channel. Typically, PAPR for the transmitted signals is $PAPR\{s(n)\} = \frac{\|s(n)\|^2}{\{\|s(n)\|^2\}}$; $0 \leq N \leq (N-1)$. Both continuous/discrete time OFDM signals with a 'L' value >4, requires PAPR reduction. The complementary cumulative distribution function (CCDF) for MIMO-OFDM is $CCDF\{PAPR_{MIMO}\{s(n)\}\} = Pr(PAPR_{MIMO}\{s(n)\} > PAPR_{AD_{THD}})$ that evaluates PAPR reduction, where $PAPR_{ADTHD}$ is an adaptive threshold. However, transmit antennas affect PAPR and hence MIMO needs effective PAPR reduction techniques.

3. PROPOSED METHOD

In this section, three different methods are proposed, which includes 1) D-UFMC-SLM, 2) M-EAAC SCS-TI and 3) DTLC, where D-UFMC-SLM is deployed in 5G UFMC system model and the other two methods are deployed in MIMO-OFDM system model.

3.1. D-UFMC-SLM

Figure 3 shows substantial PAPR reduction with D-UFMC-SLM. It emulates a UFMC system with a wide spectrum band of sub-carriers N_{sc} and M-ary encoding QAM of order 8, 16, 32, and 64 to map data bits into symbols. It generates a complex symbol pack with parallel B N-point subsequences S_b.

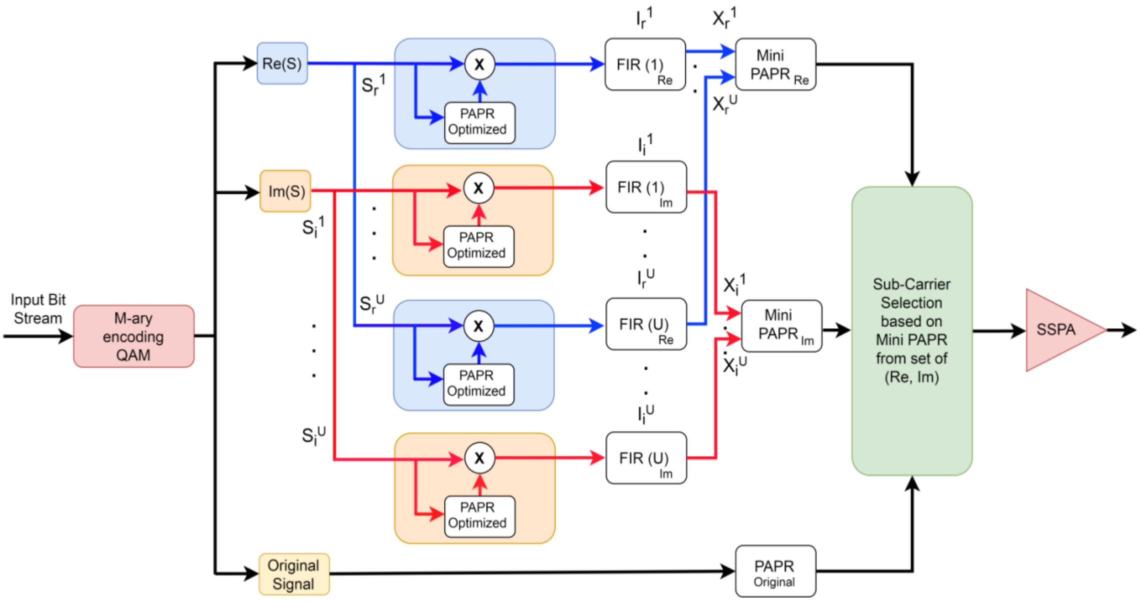

Figure 3. Block diagram of -UFMC-SLM

For maximum PAPR reduction, each component *N*-1 is phase vector-treated. This element-wise multiplication works for real and imaginary components$(I_r^U \& I_i^U)$. A matrix $S_r^U = Re\{S\} \otimes P^U S_r^U = Re\{S\} \otimes P^U$simplifies processes and the phase vector rotation (2, 4, and 6) generates signals: $X_r^U = FIR[S_r^U]$ and $X_i^U = FIR[S_i^U]$. Modified component undergoes FIR and UFMC signals are analysed to estimate PAPR. The signal transmission with minimal PAPR is expressed in (1):

$$\mathrm{PAPR} = 10\, log_{10}\left(\frac{P_{peak}}{P_{avg}}\right) = 10\, log_{10} \max_{n} \frac{[|x_n^v|^2]}{E[|x_n^v|^2]} \tag{1}$$

Average power is P_{peak} and maximum instantaneous power is P_{avg}. The Max-Min approach using D-UFMC-SLM to reduce PAPR is evaluated using the CCDF. Transmission uses minimal PAPR of a candidate symbol, i.e., CCDF as in (2):

$$x^{u'} = x^u \left\{ \underset{0 \leq u \leq U-1}{arg\_min}\left[\mathrm{PAPR}_{original}, Re\left\{\mathrm{PAPR}_{r(v)}^u\right\}, Im\, g\left\{\mathrm{PAPR}_{i(v)}^u\right\}\right]\right\} \tag{2}$$

This represents the possibility of a minimum achieving the threshold $\text{PAPR}_{u'}$. When convergence occurs, the selection criterion functions under tolerable $\text{PAPR}_{(P_0)}$ data rate v_i, therefore the computed PAPR is based on the data rate D at vD is represented as P_D. this approximation is estimated as in (3):

$$Pr\left(\text{PAPR}_{u'} > \text{PAPR}_{(p_0)}\right) \approx \left(1 - \left(1 - e^{-\text{PAPR}_{(p_0)}}\right)^{\alpha N_{sc}}\right)^{U^2} \tag{3}$$

3.2. M-EAAC SCS-TI

This method uses MIMO-OFDM PAPR reduction using a decomposition of SLM with STBC at the transmitter (as in Figure 4). IFFT separates frequency domain subblocks into time domain. Each transmit antenna handles spatial and temporal subblocks. Each transmit antenna receives the best PAPR candidate sequence. M-EAAC moved spatially and temporally over random subblocks of antenna.

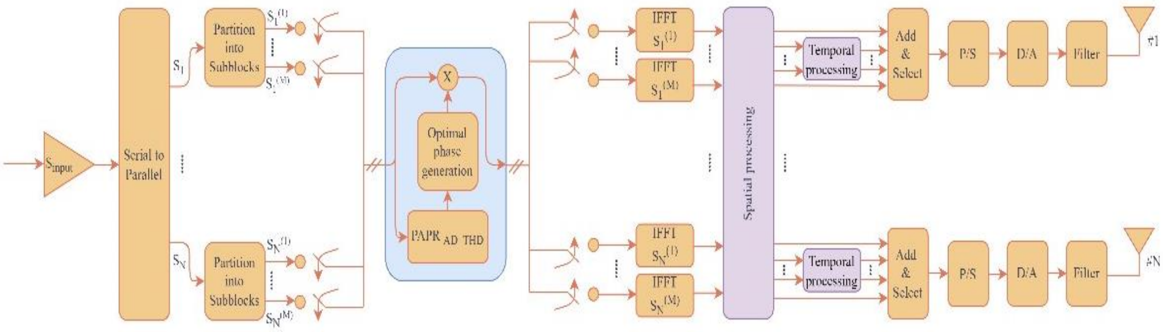

Figure 4. Proposed M-EAAC SCS-TI at transmitter side

Each broadcast antenna features spatial circular shifting subblocks and it construct numerous sequences by temporal circular shifting. The individual sequences at all transmit antenna find the lowest PAPR with possible spatial and temporal shifts while subblocks (M=4) and transmitting antennas (N=4) are used. Each transmitting antenna gets an odd subblock from a circular shift of two using odd vectors. Temporal shifting creates multiple candidate sequences and selects the lowest PAPR for signal transmission at transmitting antennas by moving even and odd subblocks. The temporal and spatial shifts of odd subblocks is expressed in (4) and (5):

$$S_{sp} = N * \left(\frac{M}{2}\right) \tag{4}$$

$$S_{tp} = \left[N * \left(\frac{M}{2}\right)\right] \cdot \left[N \cdot C^{\frac{M}{2}}\right] \tag{5}$$

Where,C represents transmission subblocks. So, temporal shift with circular shifting (Figure 5) process on even subblocks minimizes PAPR. SCS-TI creates candidate sequences with $\left[N * \left(\frac{M}{2}\right)\right] \cdot \left[N \cdot C^{\frac{M}{2}}\right]$ information bits. After separating the transmit antenna subblocks, even subblocks is obtained from temporal interleaving. Thus, an exhaustive search finds the transmit antenna sequence with the lowest PAPR.

3.3. DTLC

The DTLC determines the dynamic threshold α for each symbol based on its properties. Property based on signal median (m) and standard deviation (σ). The signal loudness controls companding and decompanding, thereby the discrete signal amplitude at MIMO-OFDM transmitter is expressed in (6):

$$|A| = \{\ |Sa|,\ 0 \leq |Sa| \leq \propto\ |Sa'|,\ |Sa| \geq \propto \tag{6}$$

Companding reduces signal amplitude based on threshold ∝. Signals compress only if their amplitude exceeds the threshold and it will compress without losing data.

Receiver gets dynamic threshold to expand/decompress and it classifies companded signals by its amplitude. Thus, the received signals beyond the threshold limit ∝ are considered compounded and expanded using (5):

$$|r'| = \propto -1 + (10|r| - \propto) \quad (7)$$

High-amplitude signal compression at the transmitter introduces the dynamic threshold ∝ ($\mu - law$ log). Offset simplifies receiver decompanding by smoothing transitions and adding the offset to the signal step helps determine the μ value.

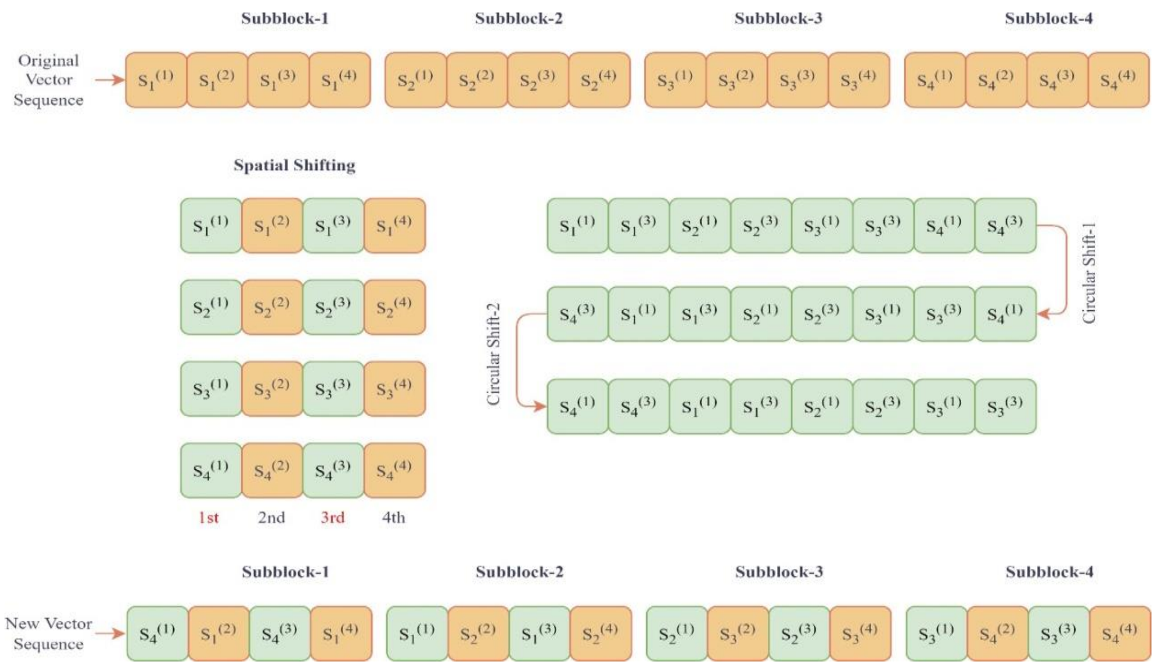

Figure 5. SCS-TI in decomposed SLM technique

4. COMPARATIVE ANALYSIS

In this section, the proposed method including 1) D-UFMC-SLM, 2) M-EAAC SCS-TI and 3) DTLC is tested over various metrics including CCDF-PAPR, Spectral Efficiency and BER in MIMO-OFDM systems. The parameters required to validate the proposed methods in Matlab simulation tool is (i) Occupied No. of sub carriers: 256,408 (ii) No. of bits transmitted: 960kbps/sec (iii) Size of FFT:1024 (iv) Length of cyclic prefix: 128 samples (v) Individual size of frame : 96 bits (vi) Modulation scheme: M-ary encoding QAM (32 & 64) (vii) Length of filter:74 (viii) Total no. of sub-bands:35 (ix) Size of sub-bands:8 (x) Power Amplifier (PA): SSPA (xi) Interleaving matrix of spatial shift:4 (x) μ: 4 - 4.5

4.1. Comparison of CCDF vs. PAPR with N = 2

In this section, the proposed D-UFMC-SLM, M-EAAC SCS-TI and DTLC methods are tested for CCDF-PAPR vs. PAPR (dB) under various transmitting antennas (say N=2) with total subblocks (M)= 8, 16 and 32. Across all scenarios (2 transmitting antennas with 8, 16, and 32 subblocks) in Figure 6, M-EAAC SCS-TI emerges as an effective method for reducing the PAPR, which shows a 15.8% reduction at 12 dB i.e., highest PAPR. DTLC also shows a performance with a reduction of 11.8%. Finally, D-UFMC-SLM lags behind M-EAAC SCS-TI and DTLC with a total reduction of 2.12%. However, variations in the sub-blocks show a minimal or no changes in the CCDF-PAPR. The results show a better performance of M-EAAC SCS-TI in reducing the PAPR over various network configurations, which shows its potential in improving the signal quality and spectral efficiency in MIMO-OFDM systems.

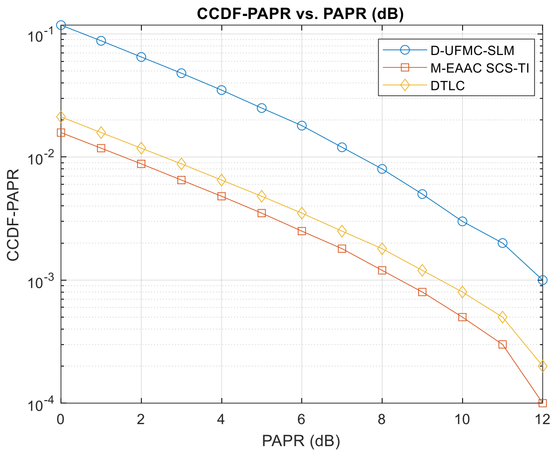

Figure 6. CCDF-PAPR vs. PAPR (dB) between: 1) D-UFMC-SLM, 2) M-EAAC SCS-TI and 3) DTLC under No. of transmitting antennas (N=2), Subblocks (M)= 8, 16 and 32

4.2. Comparison of CCDF vs. PAPR with N = 4

In this section, the proposed D-UFMC-SLM, M-EAAC SCS-TI and DTLC methods are tested for CCDF-PAPR vs. PAPR (dB) under increasing number of transmitting antennas (say N=4) with the same subblocks. Under 4 transmitting antennas with varying subblocks in Figure 7, M-EAAC SCS-TI shows a reduced CCDF-PAPR with increasing PAPR, which shows a 16.2% reduction at its highest PAPR. The DTLC shows a 12.1% and D-UFMC-SLM shows a 2.33% reduction in CCDF-PAPR, which shows its significance in optimizing the PAPR reduction for UFMC and MIMO-OFDM communication.

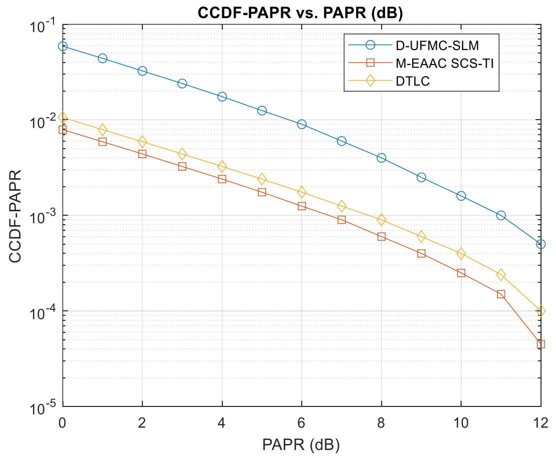

Figure 7. CCDF-PAPR vs. PAPR (dB) between: 1) D-UFMC-SLM, 2) M-EAAC SCS-TI and 3) DTLC under No. of transmitting antennas (N=4), Subblocks (M)= 8, 16 and 32

4.3. Comparison of CCDF vs. PAPR under Phase Vector

In this section, the proposed D-UFMC-SLM, M-EAAC SCS-TI and DTLC methods are tested for CCDF-PAPR vs. PAPR (dB) under various phase vectors say U = 7 and 9. The CCDF-PAPR under phase vectors for the proposed D-UFMC-SLM, M-EAAC SCS-TI, and DTLC methods is illustrated in Figure 8. For all phase vector, M-EAAC SCS-TI shows a superior performance in terms of reduced CCDF-PAPR across the spectrum than the other proposed DTLC and D-UFMC-SLM. The precise requirements of all these three models generate a better PAPR reduction, wherein M-EAAC SCS-TI is favorable to handle the MIMO-OFDM scenarios than the others. Meanwhile, the low CCDF-PAPR in all the three methods creates a balance between computational complexity and PAPR reduction. Figure 8(a) shows the under-phase vector 7 and Figure 8(b) shows the under-phase vector 9.

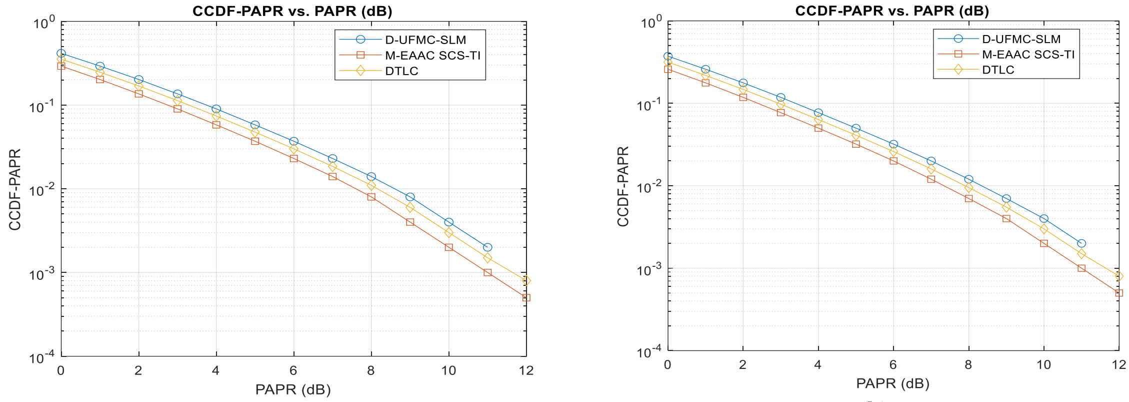

(a) (b)

Figure 8. CCDF-PAPR vs. PAPR (dB) (a) under phase vector 7 (b) under phase vector 9 between: 1) D-UFMC-SLM, 2) M-EAAC SCS-TI and 3) DTLC under various phase vector (U) with M-ary QAM encoding (=64) with Size of FFT $N_{sc} = 1024$

4.4. Comparison of BER vs. SNR under Phase Vector

In this section, the proposed D-UFMC-SLM, M-EAAC SCS-TI and DTLC methods are tested for BER vs. SNR (dB) under various phase vectors say U = 3, 5, 7, and 9. From the results of Figure 9, BER for D-UFMC-SLM, M-EAAC SCS-TI, and DTLC under different phase vectors shown in Figure 9(a), in specific U = 9 shows a significant performance. At the lower SNR levels range (say 0-4 dB), a lowest BER is achieved by M-EAAC SCS-TI, DTLC and D-UFMC-SLM shown in Figure 9(b), which shows its resilience against noise in MIMO-OFDM and UFMC environment. However, with increasing SNR, M-EAAC SCS-TI exhibits a higher performance than the other proposed DTLC and D-UFMC-SLM in high-quality transmission scenarios. The adaptive nature of these methods in complex environment shows a reduced BER with improved computational efficiency.

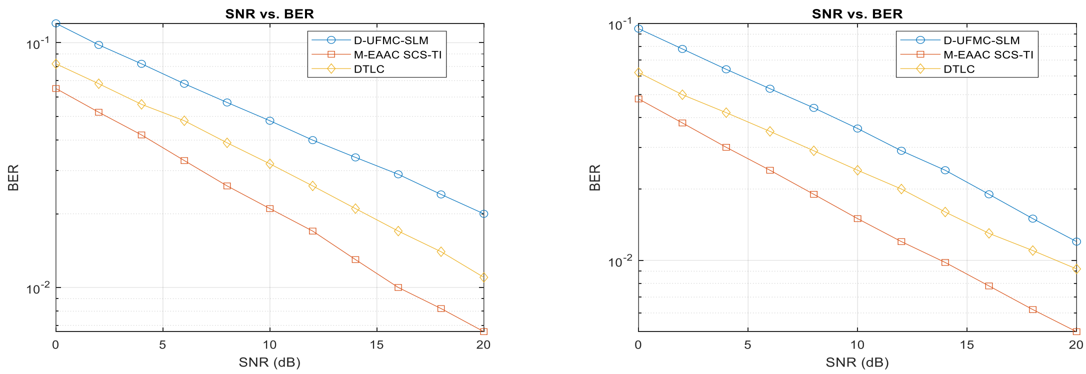

(a) (b)

Figure 9. BER vs. SNR (a) under phase vector 7 (b) under phase vector 9 between: 1) D-UFMC-SLM, 2) M-EAAC SCS-TI and 3) DTLC under various phase vector with M-ary QAM encoding with FFT Nsc = 1024

4.5. Comparison of Average Spectral Efficiency vs. SNR under various M-ary QAM

In this section, the proposed D-UFMC-SLM, M-EAAC SCS-TI and DTLC methods are tested for average spectral efficiency (ASE) vs. SNR (dB) under various QAM formats, say 32 and 64. From the results of Figure 10, average spectral efficiency (ASE) for D-UFMC-SLM, M-EAAC SCS-TI, and DTLC under varying M-ary encoding QAM shows an increasing ASE i.e., shown in Figure 10(a) especially when M-ary QAM is 64. At all SNR levels (0-20 dB), M-EAAC SCS-TI, DTLC and D-UFMC-SLM shows an increasing trend in ASE, where M-EAAC SCS-TI with its dynamic nature achieves a higher ASE than its predecessors.

This further balance the trade-off between the computational complexity and ASE in MIMO-OFDM and UFMC shown in Figure 10(b).

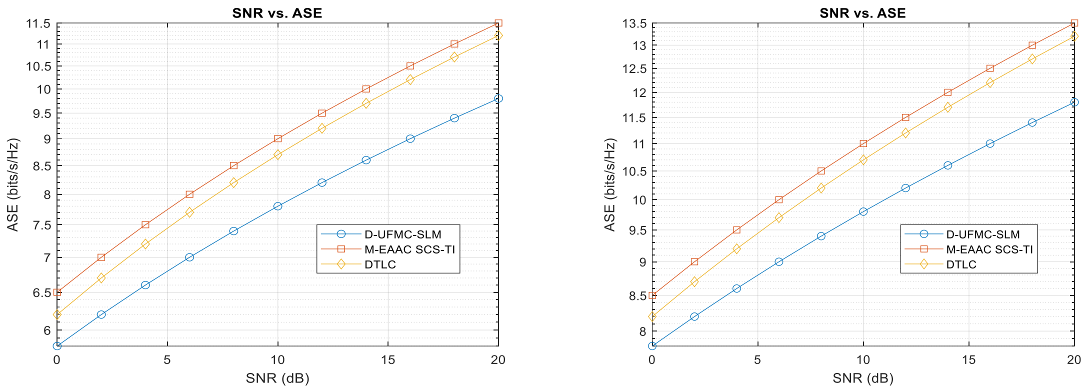

(a) (b)

Figure 10. Average Spectral Efficiency between: 1) D-UFMC-SLM, 2) M-EAAC SCS-TI and 3) DTLC) vs. SNR under M-ary encoding QAM (a)32 and (b) 64

5. CONCLUSION

In this paper, the proposed study conducts a comprehensive evaluation on all proposed methods that includes D-UFMC-SLM, M-EAAC SCS-TI, and DTLC under various metrics including BER, CCEF-PAPR and ASE in MIMO-OFDM and UFMC systems under diverse conditions. The results shows that M-EAAC SCS-TI consistently performs well on all these metrics with reduced BER, higher ASE and enhanced PAPR reduction than the other proposed methods D-UFMC-SLM and DTLC, especially under diverse phase vectors and at higher modulations. While DTLC also exhibits a slight better performance than D-UFMC-SLM, and shows its efficiency and adaptability towards both MIMO-OFDM and UFMC systems across varying channel conditions. Thus, the results offer a potential in reducing PAPR in complex channel condition and may further be tested on higher modulation schemes with increasing transmit antennas.

REFERENCES

[1] I. Jeanclaude, “Transmission Techniques for Digital Terrestrial TV Broadcasting,” *IEEE Communications Magazine*, vol. 33, no. 2, pp. 100–109, 1995, doi: 10.1109/35.350382.
[2] H. Nikookar and K. S. Lidsheim, “Random phase updating algorithm for OFDM transmission with low PAPR,” *IEEE Transactions on Broadcasting*, vol. 48, no. 2, pp. 123–128, 2002, doi: 10.1109/TBC.2002.1021278.
[3] S. B. Slimane, “Peak-to-average power ratio reduction of OFDM signals using broadband pulse shaping,” in *Proceedings IEEE 56th Vehicular Technology Conference*, IEEE, 2002, pp. 889–893. doi: 10.1109/VETECF.2002.1040728.
[4] S. H. Han and J. H. Lee, “PAPR reduction of OFDM signals using a reduced complexity PTS technique,” *IEEE Signal Processing Letters*, vol. 11, no. 11, pp. 887–890, Nov. 2004, doi: 10.1109/LSP.2004.833490.
[5] Luqing Wang and C. Tellambura, “A simplified clipping and filtering technique for PAR reduction in OFDM systems,” *IEEE Signal Processing Letters*, vol. 12, no. 6, pp. 453–456, Jun. 2005, doi: 10.1109/LSP.2005.847886.
[6] T. Jiang, W. Yao, P. Guo, Y. Song, and D. Qu, “Two novel nonlinear companding schemes with iterative receiver to reduce PAPR in multi-carrier modulation systems,” *IEEE Transactions on Broadcasting*, vol. 52, no. 2, pp. 268–273, Jun. 2006, doi: 10.1109/TBC.2006.872992.
[7] S. Yoo, S. Yoon, S. Y. Kim, and I. Song, “A novel PAPR reduction scheme for OFDM systems: Selective mapping of partial tones (SMOPT),” *Digest of Technical Papers - IEEE International Conference on Consumer Electronics*, vol. 2006, pp. 287–288, 2006, doi: 10.1109/ICCE.2006.1598423.
[8] S. Ben Slimane, “Reducing the peak-to-average power ratio of OFDM signals through precoding,” *IEEE Transactions on Vehicular Technology*, vol. 56, no. 2, pp. 686–695, 2007, doi: 10.1109/TVT.2007.891409.
[9] H. Chen and H. Liang, “PAPR reduction of OFDM signals using partial transmit sequences and Reed-Muller codes,” *IEEE Communications Letters*, vol. 11, no. 6, pp. 528–530, 2007, doi: 10.1109/LCOMM.2007.070172.
[10] J. Urban and R. Marsalek, “OFDM PAPR Reduction by Partial Transmit Sequences and Simplified Clipping with Bounded Distortion,” in *2008 18th International Conference Radioelektronika*, IEEE, Apr. 2008, pp. 1–4. doi: 10.1109/RADIOELEK.2008.4542686.
[11] M. J. Hao and C. H. Lai, “Precoding for PAPR reduction of OFDM signals with minimum error probability,” *IEEE Transactions on Broadcasting*, vol. 56, no. 1, pp. 120–128, 2010, doi: 10.1109/TBC.2009.2034512.
[12] P. Varahram, W. F. Al-Azzo, and B. M. Ali, “A low complexity partial transmit sequence scheme by use of dummy signals for PAPR reduction in OFDM systems,” *IEEE Transactions on Consumer Electronics*, vol. 56, no. 4, pp. 2416–2420, 2010, doi: 10.1109/TCE.2010.5681122.
[13] A. Ghassemi and T. Gulliver, “PAPR reduction of OFDM using PTS and error-correcting code subblocking - Transactions Papers,” *IEEE Transactions on Wireless Communications*, vol. 9, no. 3, pp. 980–989, Mar. 2010, doi: 10.1109/TWC.2010.03.061099.

[14] Hem Dutt Joshi and R. Saxena, "PAPR reduction in OFDM systems using precoding with clipping," in *2011 International Conference on Communications, Computing and Control Applications (CCCA)*, IEEE, Mar. 2011, pp. 1–5. doi: 10.1109/CCCA.2011.6031203.

[15] M. A. Aboul-Dahab, "PAPR Reduction Based on DFT Precoding for OFDM Signals," *International Journal of Future Computer and Communication*, vol. 2, no. 4, pp. 325–328, 2013, doi: 10.7763/IJFCC.2013.V2.177.

[16] S. Kaur and G. S. Saini, "Review paper on PAPR reduction techniques in OFDM system," *Indian Journal of Science and Technology*, vol. 9, no. 48, Jan. 2017, doi: 10.17485/ijst/2016/v9i48/106893.

[17] J. Hou, J. Ge, and J. Li, "Peak-to-average power ratio reduction of OFDM signals using PTS scheme with low computational complexity," *IEEE Transactions on Broadcasting*, vol. 57, no. 1, pp. 143–148, 2011, doi: 10.1109/TBC.2010.2079691.

[18] T. Arbi, I. Nasr, and B. Geller, "Near capacity RCQD constellations for PAPR reduction of OFDM systems," in *ICASSP 2020 - 2020 IEEE International Conference on Acoustics, Speech and Signal Processing (ICASSP)*, IEEE, May 2020, pp. 5110–5114. doi: 10.1109/ICASSP40776.2020.9053923.

[19] E. A. Tuli, R. Akter, J. M. Lee, and D. Kim, "Whale optimization-based PTS scheme for PAPR reduction in UFMC systems," *IET Communications*, vol. 18, no. 2, pp. 187–195, Jan. 2024, doi: 10.1049/cmu2.12708.

[20] D. Ramadevi and P. T. Rao, "PAPR reduction techniques in MIMO-OFDM communication systems," in *AIP Conference Proceedings*, 2024, p. 020016. doi: 10.1063/5.0111838.

[21] D. Ramadevi and P. Trinatha Rao, "Maximal-minimum hybrid approach with decomposed SLM technique for 5G UFMC system PAPR reduction," *Optik*, vol. 270, p. 169955, Nov. 2022, doi: 10.1016/j.ijleo.2022.169955.

[22] A. Hammoodi, L. Audah, and M. A. Taher, "Green coexistence for 5G waveform candidates: A review," *IEEE Access*, vol. 7, pp. 10103–10126, 2019, doi: 10.1109/ACCESS.2019.2891312.

[23] M. Mounir, M. B. El-Mashade, S. Berra, G. S. Gaba, and M. Masud, "A novel hybrid precoding-companding technique for peak-to-average power ratio reduction in 5g and beyond," *Sensors*, vol. 21, no. 4, pp. 1–22, 2021, doi: 10.3390/s21041410.

[24] S. A. Fathy, M. Ibrahim, S. El-Agooz, and H. El-Hennawy, "Low-complexity SLM PAPR reduction approach for UFMC systems," *IEEE Access*, vol. 8, pp. 68021–68029, 2020, doi: 10.1109/ACCESS.2020.2982646.

[25] M. I. Al-Rayif, H. E. Seleem, A. M. Ragheb, and S. A. Alshebeili, "Papr reduction in ufmc for 5G cellular systems," *Electronics (Switzerland)*, vol. 9, no. 9, pp. 1–15, 2020, doi: 10.3390/electronics9091404.

[26] H. Tiwari, R. Roshan, and R. K. Singh, "PAPR reduction in MIMO-OFDM using combined methodology of selected mapping (SLM) and partial transmit sequence (PTS)," in *2014 9th International Conference on Industrial and Information Systems (ICIIS)*, IEEE, Dec. 2014, pp. 1–5. doi: 10.1109/ICIINFS.2014.7036495.

BIOGRAPHIES OF AUTHORS

Dubala Ramadevi is a Research Scholar in the Department of Electronics and Communication Engineering, GITAM University, Hyderabad, India. She has completed her Masters in Engineering with majors in VLSI & Embedded Systems from Vasavi College of Engineering, Osmania University, India. She completed her Bachelor of Technology in Electronics and Communication Engineering from Bhoj Reddy Engineering College for women, Hyderabad, India. She can be contacted at email: dubalarama@gmail.com.

P. Trinatha Rao is a professor in the Department of Electronics and Communication Engineering, GITAM University, Hyderabad, India. He did his Ph.D. in communication networks from College of Engineering, Andhra University, Visakhapatnam, India. He has completed his masters in engineering with majors in optical communication, College of Engineering, Guindy, Chennai, India. He completed his bachelor of engineering in electronics and communication engineering from College of Engineering, GITAM, Visakhapatnam, India. He has more than 20 years of Teaching and Research Experience. Eight (8) Ph.D. degrees have been awarded under his guidance. He is presently guiding 14 research scholars in the areas of cognitive radio and software defined networks. He has published more than 85 research papers in International Journals and Conferences. He is the Editorial Board member for different Journals. He was a key note speaker in many University and Government Organizations. He has reviewed books in the area of optical fiber communications. One of the research paper titled, "Routing protocols in wireless sensor networks: a survey" has been awarded as best research paper by a renowned Journals. He was honored with Best Researcher Award-2017, received from honorable vice-president of India, Sri Venkaiah Naidu, Sri T. Harish Rao, Minister for Irrigation, Marketing and Legislative Affairs (Government of Telangana), November 18, 2017. He can be contacted at email: tpolipal@gitam.edu.